

Tailoring LPBF Process Strategies for Al₂O₃-based Ceramics: From Single Tracks to Bulk Samples Fabrication

G. Thangamani¹, A. Aversa¹, E. Padovano¹, R. Taurino², F. Bondioli¹

¹ Department of Applied Science and Technology, Politecnico di Torino, Corso Duca Degli Abruzzi 24, 10129 Torino, Italy

² Department of Industrial Engineering, University of Florence, Via di Santa Marta 3, Firenze 50139, Italy

geethapriyan.thangamani@polito.it

Abstract

Alumina (Al₂O₃) based materials have a poor laser absorptivity, high melting point, and low thermal conductivity, making them challenging materials to be processed via Laser Powder Bed Fusion (L-PBF). This study investigates the optimization of L-PBF process parameters for Al₂O₃ ceramics starting from single scan tracks (SST) to bulk samples. Initially, SSTs were produced using pure Al₂O₃, Al₂O₃-ZrO₂ eutectic, evaluating the addition of graphene as an absorption enhancer. The influence of linear energy density (LED) on track shape (width, depth), stability, and continuity was analysed, and the results revealed that zirconia and graphene, under high LED conditions, significantly improved melt pool behaviour. Subsequently, bulk samples were fabricated with different strategies to assess the surface quality, defect formation, and densification. The process parameters, such as laser power and scanning speed, were optimized. The results show that the use of an optimized 67° scanning strategy significantly improves printability while reducing thermal cracking and increasing density. This study provides valuable insights into tailoring L-PBF process parameters for Al₂O₃ based ceramics to establish a pathway towards the reliable printing of dense and crack-free Al₂O₃ ceramics suitable for high performance applications.

Keywords: Laser powder bed fusion (L-PBF), Alumina (Al₂O₃), Single Scan Track (SST), Linear Energy Density (LED), Volume Energy Density (VED), Surface Quality and Densification.

1. Introduction

Laser Powder Bed Fusion (L-PBF) is a prominent additive manufacturing technology that enables the fabrication of complex components through layer-by-layer powder consolidation. This technology is commonly used for metals and its applicability to ceramic materials, such as Al₂O₃, is still limited. This is due to their poor laser absorption, high melting points, and low thermal conductivity, which make the process challenging. Numerous investigations have examined the viability and recent developments in L-PBF processing of Al₂O₃, such as those conducted by Deckers et al. and Ullah et al. [1,2].

In L-PBF, a focused laser beam melts the material to create tracks by scanning specific areas of a thin layer of powder. The process continues with the deposition of successive layers until the final part is built. The intricate laser-material interactions have a significant impact on the printed part quality. Phase transition, Marangoni convection, heat transfer, laser absorption, and, in some cases, material evaporation and keyhole creation are important phenomena. Process variables such as build platform temperature, hatch distance, laser power, scan speed, and layer thickness also have an impact and have to be optimized (Figure 1) [3]. Moreover, according to Fan et al. [4], defects such as porosity, rough surfaces, delamination, and recoater interference can result from melt pool instabilities.

Recent research studies used single scan track (SST) to analyze the thermo-physical processes that cause melt pool instability and scan track failure in order to better comprehend and address these issues [4,5].

Pure Al₂O₃ high reflectivity, poor thermal shock resistance and poor melt flow properties continue to hinder its L-PBF processing. As a result, only a limited variety of compositions and geometries have been studied. In their studies of Al₂O₃ bulk

samples, Abdelmoula et al. reported crack formation and implied the existence of conductive melting regimes [5, 6]. In their additional analysis of consolidation behavior, Taurino et al. and Liu et al. observed that the location within the bulk samples affected the quality of the melt pool surface [7, 8].

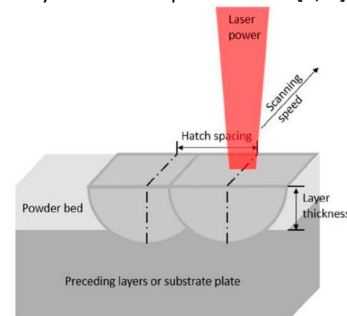


Figure 1. Schematic representation of the LPBF process (SergeiGrigoriev, et al) [13].

This study investigates the effect of process parameters and material composition on SST stability and geometry in L-PBF of Al₂O₃ (Figure 1). Two powders, such as pure Al₂O₃ and an Al₂O₃-ZrO₂-graphene eutectic mixture, were evaluated to understand the laser-powder interaction. In addition, bulk samples of the Al₂O₃-ZrO₂ eutectic mixture were fabricated to study surface morphology, defect formation, and relative density using optical and Archimedes density analyses.

2. Methodology

2.1. Material preparation

In this study pure spray-dried Al₂O₃ powder and Al₂O₃-ZrO₂ eutectic mixtures were used. The chosen zirconia powders were stabilized with 16% yttria and 0.5% graphene was added to the

eutectic mixture to enhance energy absorption as underlined in Figure 2. The obtained spherical powders (Figure 3) were sieved below 64 μm to obtain a uniform particle size distribution suitable for L-PBF.

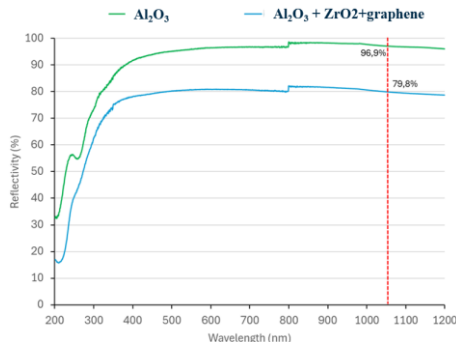


Figure 2. Laser reflectivity of Al_2O_3 -based ceramic powders. The red line indicates the wavelength of the laser in the L-PBF process.

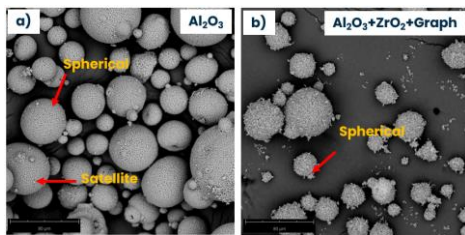


Figure 3 (a, b). Morphology of Al_2O_3 -based ceramic powders.

2.2. L-PBF setup

The powder was processed using a concept Laser Mlab system, which has a 100 W Yb fiber laser with 1064 nm wavelength and a spot size of 50 μm . The impact of process parameters, such as laser power (P) and scanning speed (v) (Table 1), on linear energy density (LED = P/v) and volumetric energy density (VED = $P/(v \times h \times t)$) was evaluated [9]. The hatch spacing (h) of 100 μm and layer thickness (t) of 40 μm were kept constant to ensure optimal uniform layer deposition and laser overlap, promoting better melt pool continuity and densification in Al_2O_3 -based ceramic L-PBF. The scan track geometry and surface continuity of SSTs and bulk samples were investigated using optical microscopy while the relative density of bulk samples by Archimedes density.

Table 1 Process parameters and their levels

Laser Power (W)	50	70	80	95
Scan Speed (mm/s)	100	200	300	400

2.3. Single Scan Track and Bulk Fabrication

SSTs were built over an Al_2O_3 baseplate of 40 mm diameter and a thickness of 10 mm with a density of 3.655 g/cm^3 . A 40 μm powder layer was spread on the platforms with a manual recoater. The baseplate with the powder bed was then placed into the machine, and 10 mm long SSTs were obtained using different process parameters. Table 1 shows the process parameters and their level for SST printed by L-PBF. SSTs were observed on top and in cross section. Track morphology and geometrical features (height- H, width – W and depth - D), under various LED conditions were assessed.

10 \times 10 mm^2 bulk samples were fabricated based on the optimal SSTs window with scanning strategies of 67° as shown in Figure 4. SEM analysis was performed on the bulk samples to evaluate surface flaws and microstructural integrity. [9, 10].

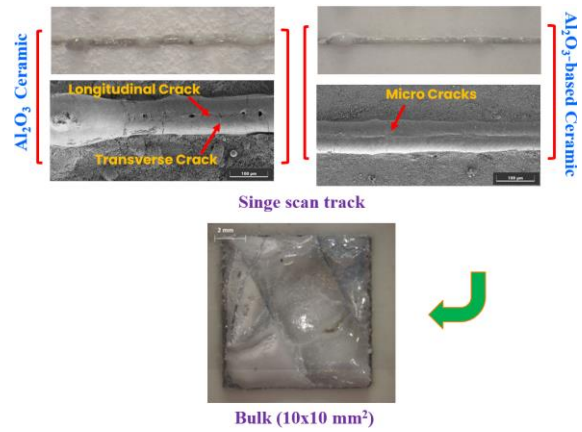


Figure 4. From L-PBF fabricated SSTs to bulk Al_2O_3 -based ceramics.

3. Results and Discussion

Three different single scan track (SST) morphologies were identified from the top-view and cross section optical micrographs: "Not enough growth," "Unstable," and "Keyholes," as illustrated in Figure 5 and 6 for laser power of 80W. The correlation between these morphologies and the building parameters is plotted in Figures 7 and 9. Figures 8 and 10 show the track width, height, and depth versus the linear energy density (LED).

The correlation between the process parameters, the SST geometrical features and the morphology suggests that keyhole SSTs are obtained with low scanning speed of about 100 mm/s due to high energy density. The unstable balling effect is observed in the moderate scanning speed range of 200 and 300 mm/s. The insufficient growth on high scanning speed 400 mm/s is due to the not sufficient time to melt the powder over the surface of the baseplate. In these conditions, the low energy density does not allow the melting of the powder, which results in scan tracks that are either absent or irregular (Figures 7 and 9).

Process parameters	Pure Al_2O_3 80W	Al_2O_3 - ZrO_2 -graphene 80W
100 mm/s		
200 mm/s		
300 mm/s		
400 mm/s		

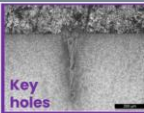
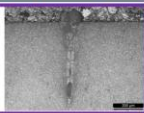
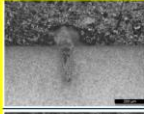
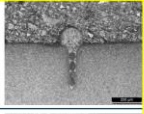
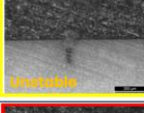
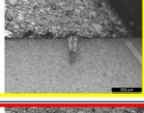
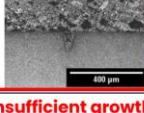
- Too thick
 - Irregular & Balling
 - Insufficient growth

Figure 5. SSTs of Al_2O_3 -based ceramics with different scanning speeds (100, 200, 300, and 400 mm/s) with laser power of 80 W.

Figures 8 and 10 show the correlation between LED and the geometrical features. At low linear energy densities (LED) the scan tracks exhibit minimal height and width, and depth values of about 100 microns. This regime typically results in "not enough growth" morphologies due to insufficient melting of the powder bed. The lack of adequate energy input leads to discontinuous tracks, indicating poor laser-material interaction and a weak bond with the substrate [10]. With a moderate increase in LED, all the dimensions of the track (H, W, D) begin to increase steadily. In this range, conduction-mode melting dominates, leading to the formation of "unstable" tracks. These tracks may appear continuous but are often asymmetric or irregular due to excessive melt pool fluctuations. This instability

arises from increased molten volume and Marangoni convection effects, as also noted by Zhang et al. (2025) in multiple alloys [9].

At higher LED levels, the track depth increases further, while the width and height remain constant. This suggests a shift toward keyhole-mode melting, where localized evaporation and deep penetration occur. While this regime enhances material densification and promotes continuous track formation, it also introduces the risk of porosity and residual stresses due to intense thermal gradients and vapor recoil pressure. These features are promising for complete melting but must be carefully controlled to prevent thermal defects.

Process parameters	Pure Al ₂ O ₃ 80W	Al ₂ O ₃ -ZrO ₂ -graphene 80W
100 mm/s	 Key holes	
200 mm/s		
300 mm/s	 Inclusions	
400 mm/s	 Not enough growth	

- Too thick - Irregular & Balling - Insufficient growth

Figure 6. Cross-sectional view of Al₂O₃-based ceramics SSTs with different scanning speeds (100, 200, 300, and 400 mm/s) with laser power of 80 W

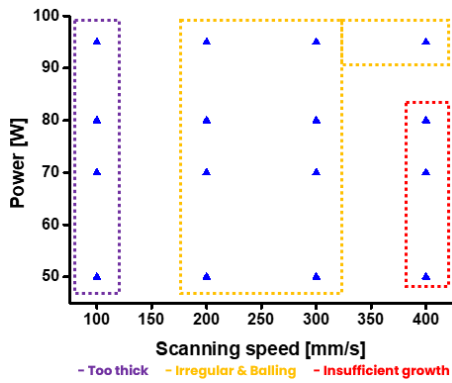


Figure 7. Laser power versus Scanning speed of Al₂O₃ SSTs.

Interestingly, Al₂O₃-ZrO₂-Graphene showed better SST tendencies than pure Al₂O₃, as shown in Figures 7 and 9. Also, the eutectic mixture powders created more stable and deeper scan tracks, particularly at similar LED values. Furthermore, eutectic mixture powders generated thicker tracks even at lower energy inputs, indicating that the graphene additions improved laser absorption [11]. For example, at 50 W and 100 mm/s, eutectic mixture samples showed thicker tracks than pure alumina, which showed thinner tracks with irregular surfaces.

Figure 4 shows that fewer defects, such as horizontal and vertical cracks, were observed in the SST of the eutectic mixture than in pure Al₂O₃ ones. Due to this, the eutectic mixture was chosen to study the printing of bulk samples.

The preliminary experiments were conducted to print bulk samples (10×10 mm²) at varying scanning speeds, as shown in Figure 11. These trials were performed using a constant laser

power of 95 W and scanning speeds of 100 mm/s and 400 mm/s. From the observations, samples printed at 100 mm/s exhibited superior surface finish and significantly fewer defects, including delamination, horizontal and vertical cracks. In the case of high scanning speed of 400 mm/s insufficient melting of the Al₂O₃-based ceramic was observed due to the rapid movement of the laser spot, leading to poor deposition and incomplete build formation.

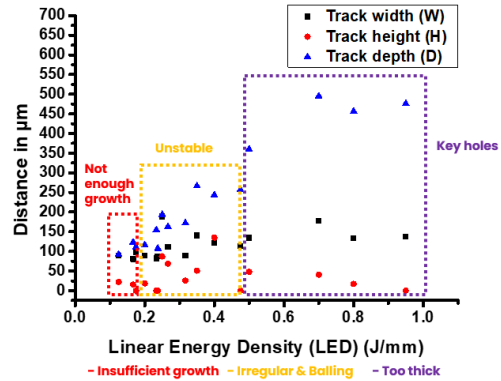


Figure 8. Linear energy density (LED) versus Distance (Track Width, height, and depth) of Al₂O₃ SSTs.

The relative density of the bulk sample printed at a scanning speed of 100 mm/s was 91.4%. For the other sample (400mm/s), density could not be determined due to poor deposition or incomplete fabrication. Therefore, a lower scanning speed of 100 mm/s resulted in better-quality bulk samples.

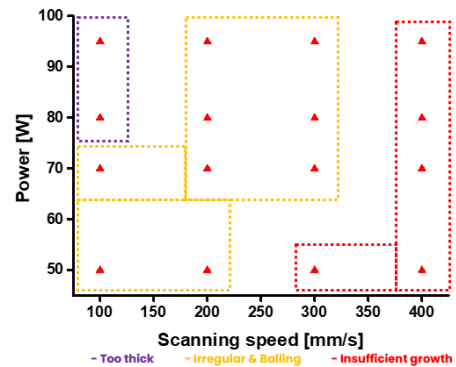


Figure 9. Laser power versus Scanning speed of Al₂O₃-ZrO₂-Graphene SSTs.

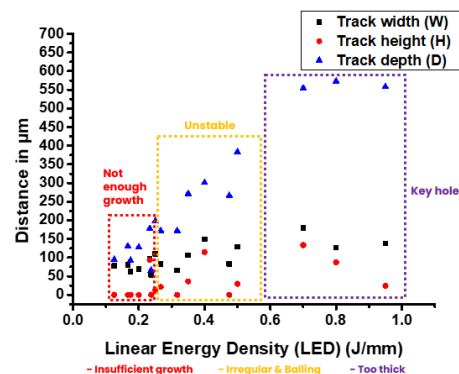


Figure 10. Linear energy density (LED) versus Distance (Track Width, height, and depth) of SSTs of Al₂O₃-ZrO₂-Graphene powders.

A constant scanning speed of 100 mm/s was used to print bulk samples (10×10 mm²) using laser powers of 50, 70, 80, and 95 W. Figure 12 shows the top surfaces of the obtained samples. Relative densities at 80 W reached 93.1% for 10×10 mm² bulk samples, indicating that densification is best achieved at

intermediate power levels [12]. These results demonstrate that the relationship between powder behavior, laser energy, and relative density need to be further investigated, particularly in the case of eutectic mixture.

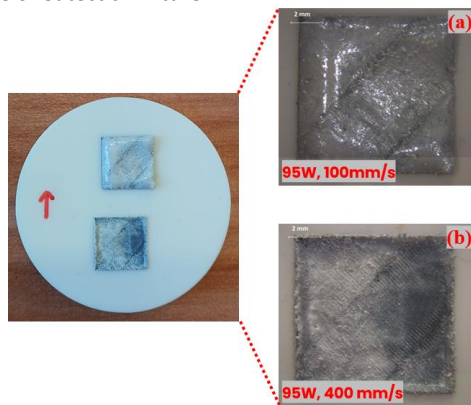


Figure 11. Bulk ($\text{Al}_2\text{O}_3\text{-ZrO}_2\text{-Graphene}$) samples ($10\times 10\text{mm}^2$) printed with a constant laser power of 95W and with different scanning speed of (a) 100 and (b) 400 mm/s.

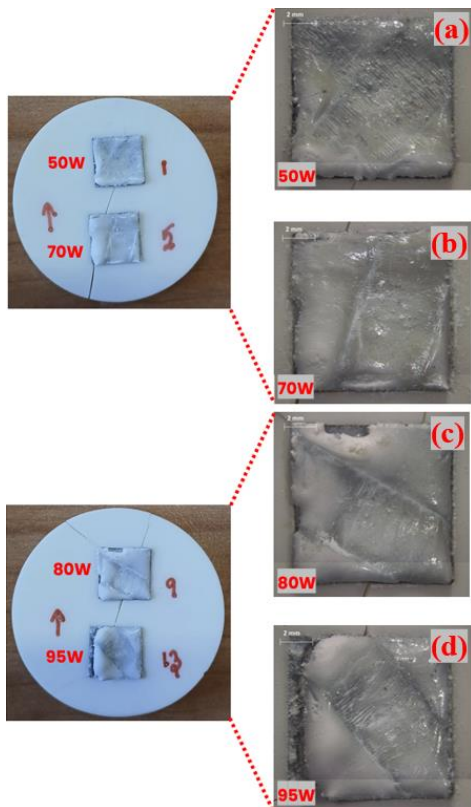


Figure 12. Bulk ($\text{Al}_2\text{O}_3\text{-ZrO}_2\text{-Graphene}$) samples ($10\times 10\times 1\text{mm}^3$) printed with a constant scanning speed of 100 mm/s with different laser powers of (a) 50, (b) 70, (c) 80, and (d) 95 W.

4. Conclusions

This work examined the impact of laser processing parameters, specifically laser power and scanning speed, on the consolidation and morphology of single scan tracks (SSTs) and bulk Al_2O_3 -based ceramics obtained by L-PBF. The results are as follow:

- Based on combinations of laser power and scanning speed, the three main SST morphologies were found:
 - "Not enough growth" with low LED input because of inadequate substrate wetting and poor melting.
 - "Unstable" morphology at moderate LED input, with asymmetric or discontinuous tracks, results in balling and uneven flow.

- "Keyhole" creation at high LED input, characterised by deep melt pools and possible vaporization effects.
- Process windows, which were built analyzing the SST morphologies, assisted in determining the suitable range of laser parameters to prevent under-melting or overheating, that provides a rapid screening tool for new material compositions
- Compared to pure Al_2O_3 , the eutectic mixture powders (Al_2O_3 with ZrO_2 and graphene) created more stable and deeper scan tracks due to a superior laser absorption, particularly at similar LED values.
- Bulk samples ($10\times 10\text{mm}^2$) were successfully printed utilizing the scanning strategy 67° at a constant scanning speed of 100 mm/s over a range of laser strengths (50–95 W).
- The highest relative densities of 93.1% were observed at 80 W, confirming that this power setting was optimal in the given condition. Densification decreased at both lower and higher laser powers due to insufficient melting and excessive thermal input.

Acknowledgments

This study was carried out within the « Dense Eutectic Ceramic Oxide by Additive Manufacturing; Sustainable by Design Materials and Technologies (ECOBAM) » project – funded by European Union – Next Generation EU within the PRIN 2022 PNRR program M4C2 CUP E53D23017820001 (DD1409 of 14/09/2022 Ministry of University and Research). This manuscript reflects only the authors' views and opinions and the Ministry cannot be considered responsible for them

References

- [1] Deckers J, Vleugels J and Kruth J P 2014 Additive manufacturing of ceramics: A review J. Ceram. Sci. Technol. **5** 245-60.
- [2] Ullah A, Shah M, Ali Z, Asami K, Ur Rehman A and Emmelmann C 2025 Additive manufacturing of ceramics via the laser powder bed fusion process Int. J. Appl. Ceram. Technol. **22** e15087.
- [3] Florio K, Puccio D, Viganò G, Pfeiffer S, Verga F, Grasso M, Colosimo B M, Graule T and Wegener K 2021 . Process characterization and analysis of ceramic powder bed fusion Int. J. Adv. Manuf. Technol. **117** 2105-16.
- [4] Fan Z, Lu M and Huang H 2018 Selective laser melting of alumina: A single track study Ceram. Int. **44** 9484-93
- [5] Abdelmoula M, Küçüktürk G, Juste E and Petit F 2022 Powder bed selective laser processing of alumina: Scanning strategies investigation Appl. Sci. **12** 764
- [6] Abdelmoula M, Küçüktürk G, Juste E and Petit F 2024 Enhancing powder bed fusion of alumina ceramic material: a comprehensive study from powder tailoring to mechanical performance evaluation Int. J. Adv. Manuf. Technol. **131** 1745-67
- [7] Taurino R, Martinuzzi S, Padovano E, Caporali S and Bondioli F 2024 Laser additive manufacturing of Al_2O_3 and ZrO_2 -based eutectic ceramic oxide: An overview J. Eur. Ceram. Soc. 117133
- [8] Liu H, Jiang H, Chen Q, Shen Z, Zhang X, Liu H and Su H 2024 Insights into the applicability of laser energy density in directly preparing Al_2O_3 -based eutectic ceramics by laser additive manufacturing Ceram. Int. **50** 3381-87
- [9] Zhang M, Fang B and Fan L 2025 Optimizing powder morphology and scanning strategies to enhance shape accuracy in L-PBF alumina ceramic formation Ceram. Int. **51** 8042-53
- [10] Liu Q, Danlos Y, Song B, Zhang B, Yin S and Liao H 2015 Effect of high-temperature preheating on the selective laser melting of yttria-stabilized zirconia ceramic J. Mater. Process. Technol. **222** 61-74
- [11] Verga F, Borlaf M, Conti L, Florio K, Vetterli M, Graule T, Schmid M and Wegener K 2020 Laser-based powder bed fusion of alumina toughened zirconia Addit. Manuf. **31** 100959
- [12] Özmen E, Grossin D, Lenormand P and Bertrand G 2025 Direct powder bed selective laser processing of dense alumina-toughened zirconia parts Prog. Addit. Manuf. **10** 2369-81
- [13] Grigoriev, S., Tarasova, T., Gusarov, A., Khmyrov, R. and Egorov, S., 2019. Possibilities of manufacturing products from cermet compositions using nanoscale powders by additive manufacturing methods. Mater., **12**(20), p.3425.